LA-UR-15-22337
Approved for public release; distribution is unlimited.

Title: Thermophysical property measurement and characterization of glass ceramic waste forms

Author(s): Tang, Ming

Intended for: DOE-Office of Nuclear Energy-milestone report

Issued: 2015-04-01

Thermophysical property measurement and characterization of glass ceramic waste forms

Fuel Cycle Research & Development

Prepared for
U.S. Department of Energy
Material Recovery & Waste Form Development Campaign

Ming Tang
Los Alamos National Laboratory

September 30, 2014

FCRD-SWF-2014-000251

Name/Title of Deliverable/Milestone	Thermophysical property measurement and characterization of glass ceramic waste forms **M3FT-14LA0308031**
Work Package Title and Number	Advanced Waste Form (Glass Ceramic)-LANL **FT-14LA030803**
Work Package WBS Number	**1.02.03.08**
Responsible Work Package Manager	Ming Tang *(Name/Signature)*
Date Submitted	*09/30/2014*

Quality Rigor Level for Deliverable/Milestone

☒ *Rigor Level 3* ☐ *Rigor Level 2* ☐ *Rigor Level 1* ☐ *Nuclear Data*

This deliverable was prepared in accordance with *Ming Tang* *(Participant's Name)*

QA program which meets the requirements of

☐ *DOE Order 414.1* ☐ *NQA-1-2000*

This Deliverable was subjected to:

☒ *Independent Technical Review* ☐ *Peer Review*

Independent Technical Review (ITR)

Review Documentation Provided

☐ *Signed ITR Report or,*

☐ *Signed ITR Concurrence Sheet or,*

☒ *Signature of ITR Reviewer(s) below*

Peer Review (PR)

Review Documentation Provided

☐ *Signed PR Report or,*

☐ *Signed PR Concurrence Sheet or,*

☐ *Signature of PR Reviewer(s) below*

Name and Signature of Peer Reviewers(s)/Independent Technical Reviewer(s)

Osman Anderoglu

SUMMARY

The research conducted in this work package is to collect data in support of future development of glass ceramic waste forms and to help develop the next generation high performance waste management technologies. This work package collaborates closely with the work conducted under “Advanced Waste Forms (Glass Ceramics) – Pacific Northwest National Laboratory (PNNL) - (FT-14PN030804)” and “Advanced Waste Forms (CCIM) – Idaho National Laboratory (INL) – (FT-14IN030807)”.

The Los Alamos National Laboratory (LANL) is focusing on characterization, thermal stability and radiation stability testing procedures on glass ceramics from the test matrix and melter testing to further develop the glass ceramic waste form for immobilization of high level waste (HLW) raffinate stream. In Fiscal Year 2014, we are mainly working on multiphase glass ceramic waste forms and single phase oxyapatite material. Various characterization techniques (including X-ray diffraction, transmission electron microscopy, scanning electron microscopy, synchrotron X-ray) were used to characterize these samples. Thermal properties including thermal conductivity, thermal diffusivity, specific heat capacity, were measured using DSC-TGA, Dilatometer, and Laser Flash techniques. For the radiation stability test, selected glass ceramic samples were exposed to either heavy ion (Kr) or light ion (He) radiations environments at elevated temperatures to test temperature effect on their radiation stability.

CONTENTS

SUMMARY 1

1. Thermal properties measurement of melter test glass ceramics 4

2. Synchrotron Micro-X-ray Diffraction and X-ray fluorescence for multiphase glass ceramics 6

3. Radiation stability test at elevated temperatures 8
   - 3.1 600 keV Kr irradiations at 250 °C 8
   - 3.2 200 keV He irradiations at 450 °C 9

4. Radiation stability on single phase oxyapatite & oxyapatite phase in multiphase waste form 11
   - 4.1 Kr irradiations on single phase oxyapatite & oxyapatite phase in multiphase waste form 11
   - 4.2 TEM/electron irradiations on single phase oxyapatite & oxyapatite phase in multiphase waste form 12
   - 4.3 Radiation stability test on single phase oxyapatite under Kr irradiations at different temperatures 13
   - 4.4 Radiation stability test on single phase oxyapatite under He irradiations at different temperatures 14

5. Future Work 15

References 16

FIGURES

Figure 1. Specific heat capacity as a function of temperature... 4

Figure 2. Thermal diffusivity as a function of temperature... 5

Figure 3. Thermal conductivity as a function of temperature. 5

Figure 4. (a) The original micro X-ray diffraction pattern, (b) XRD pattern in θ-2θ scan.. 7

Figure 5. XRD patterns of micro XRD measurement and single phase oxyapatite.. 7

Figure 6. Microfluorescence elemental mapping of sample 1XSC. 8

Figure 7. XRD results of multiphase glass ceramic samples before and after 600 keV Kr irradiations at 250 °C, (a) Mo-6.25, (b) GC-4, (c) 1XSC. 9

Figure 8. XRD results of multiphase glass ceramic samples before and after 200 keV He irradiations at 450 °C, (a) Mo-6.25, (b) GC-4, (c) 1XSC 10

Figure 9. (a) Cross-sectional TEM micrograph of oxyapatite phase in Mo-6.25 multiphase ceramic waste form irradiated with 600 keV Kr ions to a fluence of 5×10^{14} Kr/cm^2 (~1 dpa) and SAED patterns corresponding to irradiated layer and unirradiated area, respectively. (b) Cross-sectional TEM micrograph of single phase oxyapatite irradiated with 600 keV Kr ions to a fluence of 5×10^{14} Kr/cm^2 (~1 dpa) and inset SAED patterns corresponding to irradiated layer and unirradiated area, respectively 12

Figure 10. (a) High resolution transmission electron microscopy image of oxyapatite phase in multiphase glass ceramic Mo-6.25 before (left) & after (right) electron irradtion including FFT diffraction; (b) High resolution transmission electron microscopy image of single phase oxyapatite before (left) & after (right) electron irradtion including FFT diffraction.... 13

Figure 11. XRD results of single phase oxyapatite before & after 600 keV Kr irradiations at different temperatures (a) room temperature, (b) 250 °C.... 14

Figure 12. (a) XRD results of single phase oxyapatite before & after 5 MeV He irradiations at room temperature; (b) XRD results of single phase oxyapatite before & after 200 keV He irradiations at room temperature and 250 °C. 15

1. Thermal properties measurement of melter test glass ceramics

Accurate thermophyical properties (thermal conductivity, heat capacity, thermal diffusivity) as a function of temperature are critical to engineering analysis of nuclear materials including nuclear energy waste forms. These properties are important in determining the thermal gradients in a waste form during its fabrication, storage, transport and geological disposal. Thermophysical properties of glass ceramic waste forms provide very useful information on the glass melting, forming process, and crystalline phase formation.

The thermophysical properties of two Cold Crucible Induction Melting (CCIM) melter test glass ceramic waste form samples were investigated at LANL. Thermal properties including thermal conductivity, thermal diffusivity, specific heat capacity, were measured using DSC-TGA, Dilatometer, and Laser Flash (LFA) techniques from room temperature to 1000 °C. These two samples were fabricated under different cooling routes, one labeled as “Natural AM” which is under natural cooling process, another labeled as “1XSC” which is under slow cooling process. Figure 1, 2, and 3 show the specific heat capacity, thermal diffusivity and thermal conductivity as a function of temperature, respectively.

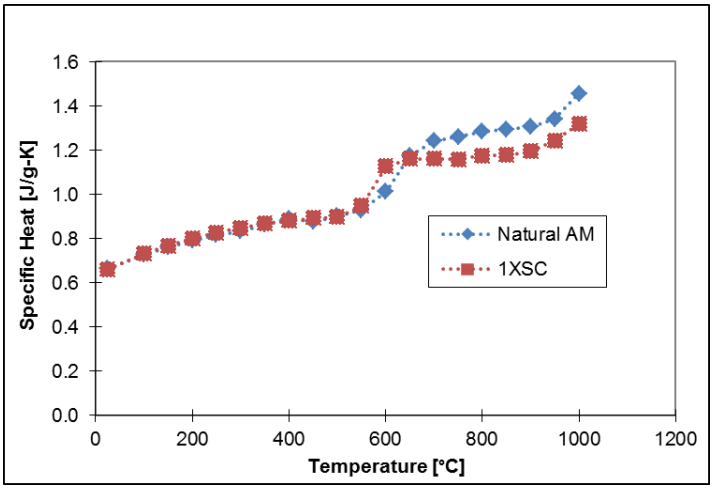

Figure 1. Specific heat capacity as a function of temperature.

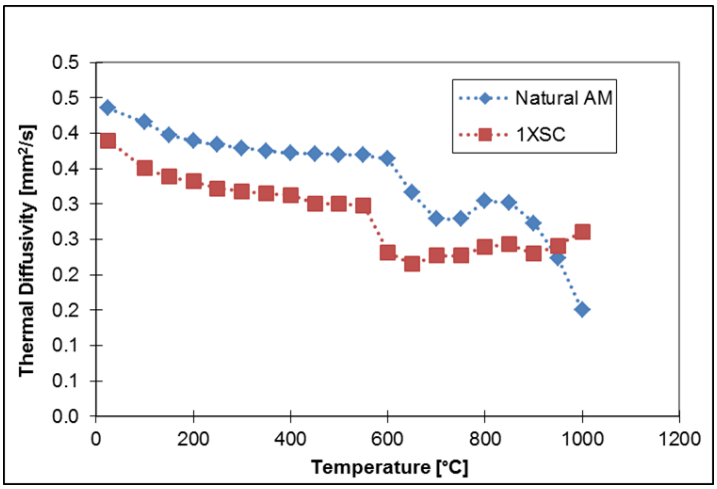

Figure 2. Thermal diffusivity as a function of temperature.

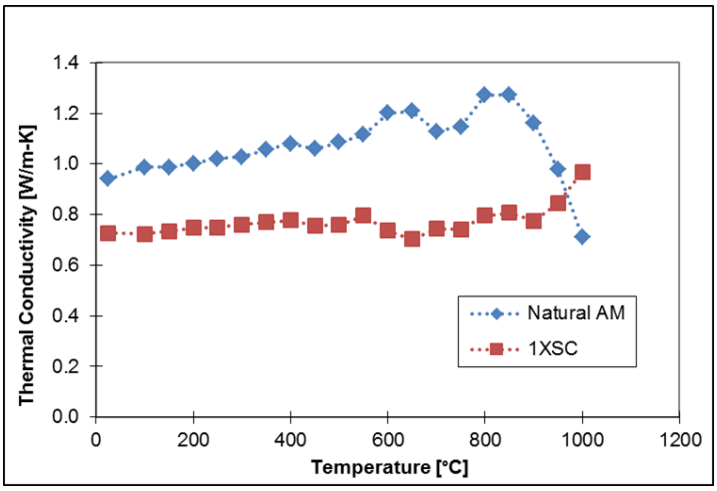

Figure 3. Thermal conductivity as a function of temperature.

The calculated heat capacity curves are shown in Figure 1, and the clear melting of a constituent (glass) within these two samples is indicated by the onset in the 580 to 620 °C range. The second glass transition begins at ~ 900 °C. Figure 2 summarizes the LFA data collected for these two samples in this work. The most pronounced feature of this plot is again the rapid decrease beginning at roughly 550°C. Both samples exhibit drastic reductions in the thermal diffusivity beginning around 550°C before stabilizing; then the thermal diffusivity of 1XSC sample gradually increases from 600°C to the peak temperature investigated in this study, while natural AM sample shows another reduction from 800°C to 1000°C. Finally, the product of the density, specific heat capacity, and thermal diffusivity was calculated to determine the thermal conductivity of both compositions. The results are shown in Figure 3, in which 1XSC sample

exhibits increasing thermal conductivity with temperature as expected for systems dominated by glasses. This behavior is attributed to the fact that the phonon mean free path in amorphous systems is constant as a function of temperature; the thermal conductivity as a function of temperature is therefore dictated by the gradually increasing heat capacity. However, natural AM sample undergoes two reductions in the thermal conductivity. The first reduction is between 650 and 750 °C, and the second continuous reduction starts 800°C to the peak temperature 1000°C. These drops are consistent with what would be expected for a system with a small fraction of liquid phase present in a solid matrix.

To evaluate thermal properties of melter test glass ceramics, we compare the data of 1XSC and natural AM samples with lab fabricated glass ceramic samples GC-4, Mo-6.25 [1] which were measured using the same techniques. It is obvious that the thermal conductivity of melter test glass ceramics is lower than that of GC-4 and Mo-6.25 samples. The amorphous glass phase fractions present in these compositions have been shown to largely dominate response. However, a more accurate understanding of the phases present as well as their individual thermophysical properties would be necessary to apply a more rigorous analysis of their individual contribution.

2. Synchrotron Micro-X-ray Diffraction and X-ray fluorescence for multiphase glass ceramics

To identify crystal structure and elemental distribution information of individual crystalline phase in multi-phase samples, advanced characterization techniques including micro-X-ray diffraction (XRD) and X-ray fluorescence at APS, were used in our CCIM melter test multi-phase glass ceramic waste form sample 1XSC. Figure 4 and 5 shows an example of micro-XRD pattern (black) from one grain in multi-phase glass ceramic labeled “1XSC”. Figure 4 (a) is the original diffraction pattern obtained from the 2-ID-D/E beamline, and (b) is the (a) pattern in θ-2θ scan. After the adjustment of energy of X-ray, this pattern is plotted in Figure 5, and it could be indexed as oxyapatite ($Ca_2Nd_8Si_6O_{26}$) phase. If we compare this synchrotron micro-XRD pattern with lab XRD measurement from a single phase oxyapatite, these two XRD patterns are almost same except some disparity of intensity.

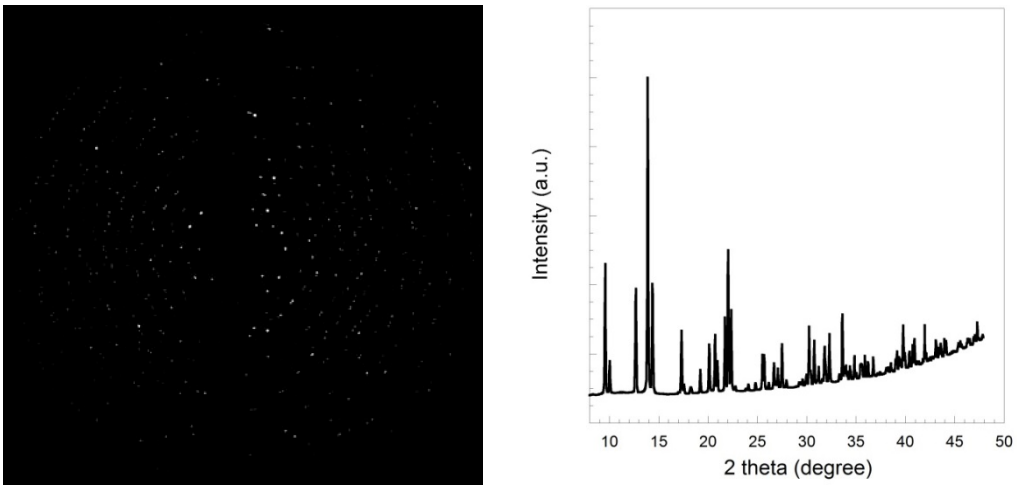

(a) (b)

Figure 4. (a) The original micro-X-ray diffraction pattern, (b) XRD pattern in θ-2θ scan.

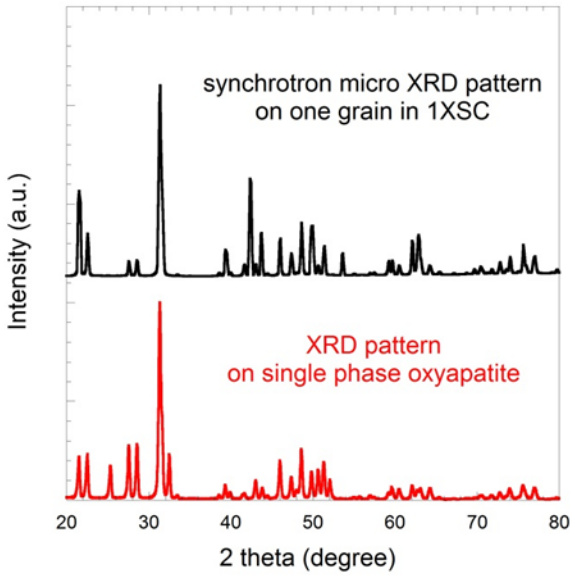

Figure 5. XRD patterns of micro XRD measurement and single phase oxyapatite.

Figure 6 shows the elemental mapping result for one grain in glass ceramic 1XSC using microfluorescence technique. This approach has successfully revealed composition structures in the differential analyses on the X-ray fluorescence images of multi-phase glass-ceramics. This mapping result shows better resolution and reveals more detail information than that of SEM/EDS. These preliminary results could demonstrate that micro-XRD and microfluorescence might be great tools to characterize multi-phase samples.

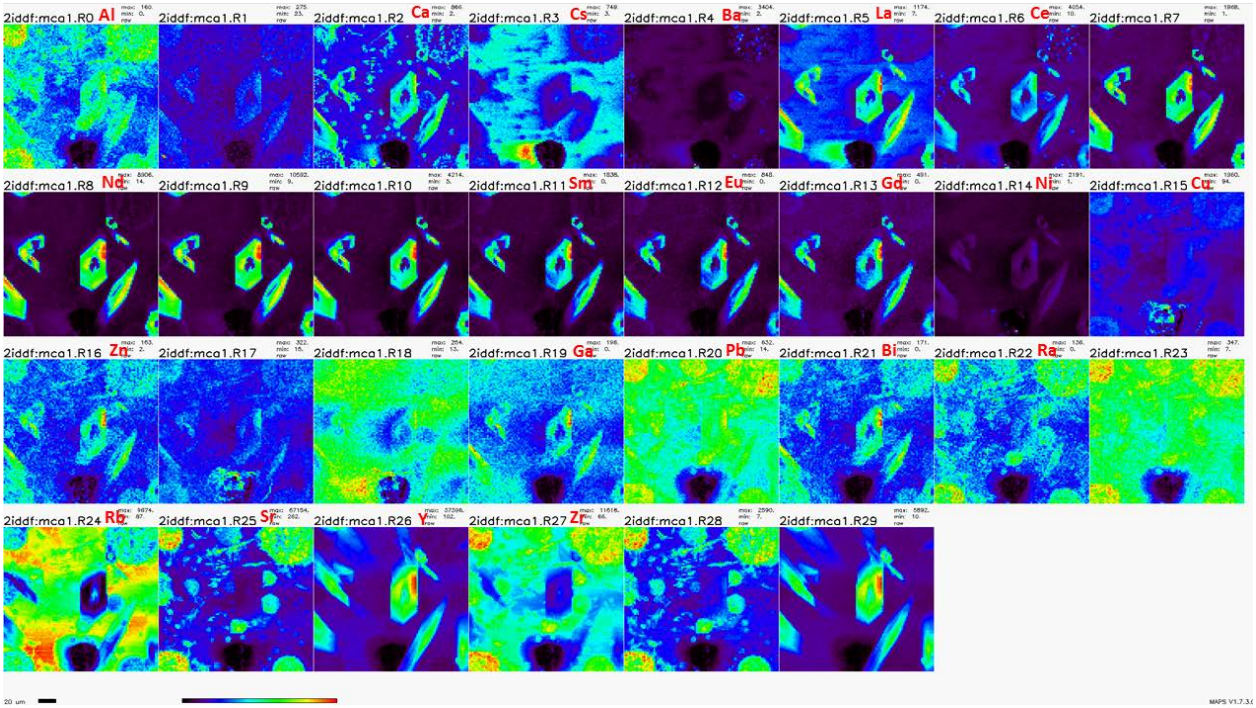

Figure 6. Microfluorescence elemental mapping of sample 1XSC.

3. Radiation stability test at elevated temperatures

LANL performed a series of ion irradiations on glass ceramic waste form samples at two elevated temperatures: (1) 250 °C, and (2) 450 °C, in an effort to simulate decay heats representative of different radionuclide loadings of a waste form. Another objective is to evaluate the temperature effect on radiation stability of glass ceramic waste forms. Our goal is to identify structural evolutionary changes that occur due to the combination of ion irradiation and elevated temperature. In this task, two kinds of lab fabricated glass ceramic samples including GC-4 and Mo-6.25 and one melter test glass ceramic sample 1XSC, were exposed to 200 keV He or 600 keV Kr ion irradiations at the above temperatures.

3.1 600 keV Kr irradiations at 250 °C

Figure 7 shows the GIXRD patterns of GC-4, Mo-6.25, and 1XSC before & after 600 keV Kr irradiations at 250 °C. The ion irradiation dose is corresponding to ~ 5 displacements per atom (dpa) calculated using SRIM simulation. Figure 7(a), (b), (c) correspond to Mo-6.25, GC-4, and 1XSC samples, respectively. GIXRD patterns reveal that the amorphous fraction in these three samples is qualitatively increased due to the ion irradiation. However, if we compare this data with previous results at room temperature irradiation [2], irradiation-induced amorphization at

250 °C is much less than that at room temperature. Obviously, most of the irradiation-induced defects are annihilated at this temperature.

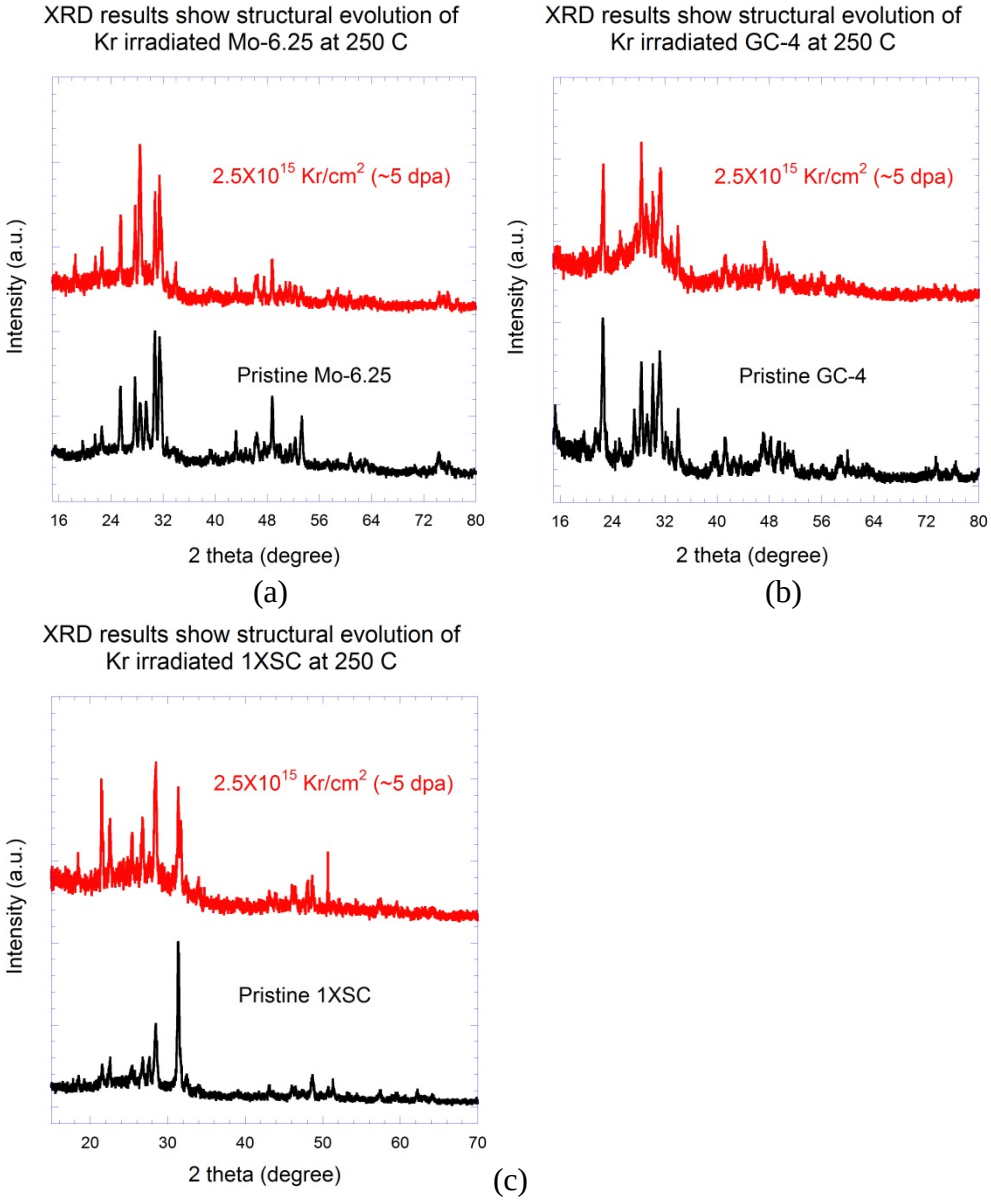

Figure 7. XRD results of multiphase glass ceramic samples before and after 600 keV Kr irradiations at 250 °C, (a) Mo-6.25, (b) GC-4, (c) 1XSC.

3.2 200 keV He irradiations at 450 °C

Figure 8 shows the GIXRD patterns of GC-4, Mo-6.25, and 1XSC before & after 200 keV Kr irradiation at 450 °C. The ion irradiation dose is corresponding to ~ 5 dpa. Figure 8(a), (b), (c) correspond to Mo-6.25, GC-4, and 1XSC samples, respectively. GIXRD patterns reveal there is

no appreciable change in microstructure before and after irradiations at 450 °C. It suggests that the radiation damage is almost fully recovered at this temperature. As mentioned early, the X-ray diffraction patterns collected from these samples are quite complex because of the multiple phases and high number of reflections in the patterns. Small changes in peak locations and intensities in these three samples suggest that the ion irradiation induces texturing of certain crystalline phases.

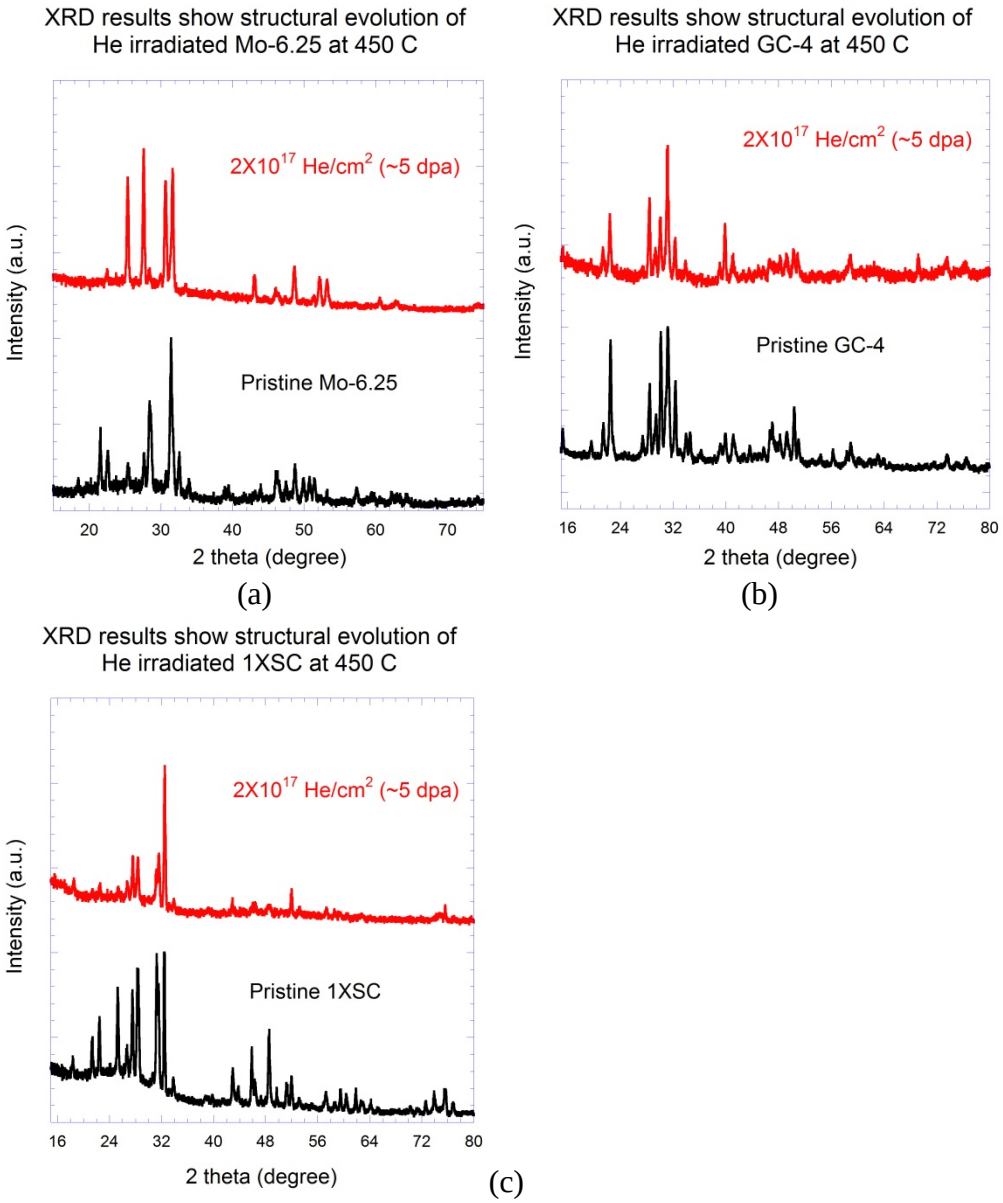

Figure 8. XRD results of multiphase glass ceramic samples before and after 200 keV He irradiations at 450 °C, (a) Mo-6.25, (b) GC-4, (c) 1XSC.

In summary, the annihilation or recombination of radiation-induced defects is accelerated at elevated temperatures, so glass ceramic waste forms show better radiation tolerance. However, their stability may be rate dependent which may limit the waste loading that can be employed.

4. Radiation stability on single phase oxyapatite & oxyapatite phase in multiphase waste form

Natural apatites, $Ca_{10}(P_{O4})_6(OH,Cl,F)_2$, are the most abundant of the phosphate minerals and are often used for age dating because of incorporated uranium. Rare-earth phosphate-silicate phases with structures analogous to natural apatite have been observed in glass-ceramic waste forms and as recrystallized alteration products on the surfaces of HLW glasses as a result of aqueous corrosion [3-5]. Rare-earth silicates with the apatite structure also have been observed as actinide host phases in a devitrified borosilicate HLW glass, a multiphase ceramic waste form, a glass-ceramic waste form, and a cement waste form. Oxyapatite ($Ca_2Ln_8Si_6O_{26}$) is becoming prominent at higher waste loading for the glass ceramic waste forms that include alkaline/alkaline earth + lanthanide + transition metal (CS+Ln+TM) fission products [6].

Radiation effects in apatite compounds, specifically for natural minerals, fluorapatite, and synthetic apatites, have been extensively studied for different types of irradiation sources [7-9]. The irradiation-induced crystalline-to-amorphous transition in apatite structure was observed under ballistic damage environment. In order to explore radiation tolerance of oxyapatite phase in multiphase glass ceramic waste forms and compare to the single phase oxyapatite, a systematic study of ion-irradiation-induced amorphization in single phase $Ca_2Nd_8Si_6O_{26}$ and $Ca_2Ln_8Si_6O_{26}$ in multiphase glass ceramic waste form was undertaken to investigate the dependence of amorphization on ion species, temperature and energy.

4.1 Kr irradiations on single phase oxyapatite & oxyapatite phase in multiphase waste form

Single phase oxyapatite $Ca_2Nd_8Si_6O_{26}$ and multiphase glass ceramic Mo-6.25 samples were subjected to a 600 keV Kr (heavy ion) beam radiations at room temperature. For multiphase samples, the EDS results under scanning transmission electron microscope (STEM) mode were used to identify the crystalline phase composition, and electron diffraction studies were used to determine their corresponding crystal structures. TEM results in Figure 9 show that oxyapatite phase in Mo-6.25 (left) is susceptible to radiation-induced amorphization at a fluence of 5×10^{18} ions/m^2 (corresponding to a dose of 1 dpa), and single phase oxyapatite (right) shows the similar

radiation response. This result is consistent with the previous studies on apatite structure materials with various compositions. Since Kr irradiation is used to simulate the alpha decay effects for nuclear waste, 1 dpa is roughly equivalent to cumulative dose of 10^{19} alpha decays/g, or 10^{21} alpha decays/m^2. 10^{19} alpha decays/g is also equivalent to 10000 years waste storage time with 5wt% ^{239}Pu loading.

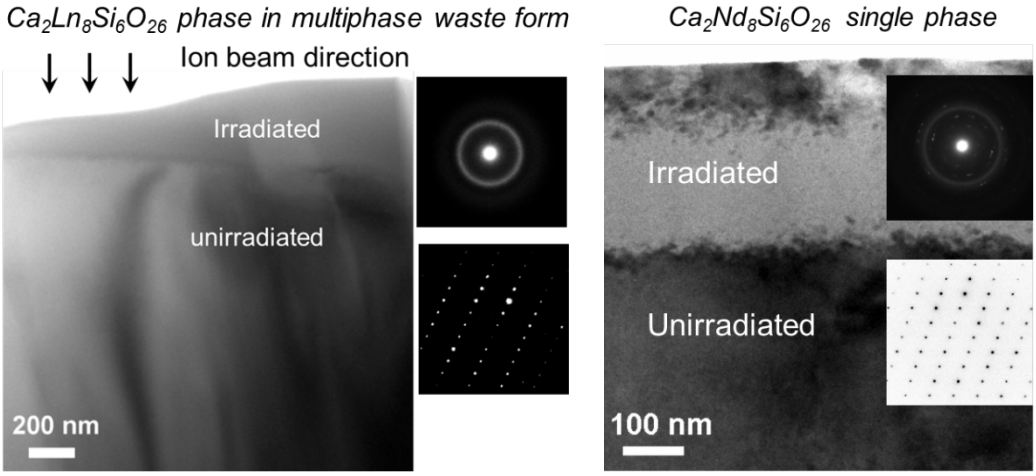

Figure 9. (a) Cross-sectional TEM micrograph of oxyapatite phase in Mo-6.25 multiphase ceramic waste form irradiated with 600 keV Kr ions to a fluence of 5 ×10^{14} Kr/cm^2 (~1 dpa) and SAED patterns corresponding to irradiated layer and unirradiated area, respectively. (b) Cross-sectional TEM micrograph of single phase oxyapatite irradiated with 600 keV Kr ions to a fluence of 5 ×10^{14} Kr/cm^2 (~1 dpa) and inset SAED patterns corresponding to irradiated layer and unirradiated area, respectively.

4.2 TEM/electron irradiations on single phase oxyapatite & oxyapatite phase in multiphase waste form

To simulate the beta and gamma radiations in a waste form incorporating fission products, *in-situ* electron beam irradiation in a TEM provide a useful means to examine radiolysis effects because they deposit nearly all of their energy in solids via electronic loss processes, which is the same energy transfer mechanism as beta and gamma radiation. Figure 10 (a) and (b) show the results of the TEM/electron irradiation study for the single phase oxyapatite $Ca_2Nd_8Si_6O_{26}$ and the oxyapatite phase ($Ca_2Ln_8Si_6O_{26}$) in glass ceramic Mo-6.25. High resolution TEM images and inset fast Fourier transforms (FFT) indicate oxyapatite phases in both samples, maintain the same apatite structure after a radiation dose of 10^{13} Gy (dose calculation using SRIM [10]). The results suggest that the oxyapatite phase exhibits stability to 1000 years at anticipated doses (2×10^{10}-

2×10^{11} Gy) [11]. It is noted that actual self-radiation during waste form storage would come from β-particle fluxes that are orders of magnitude lower than those used in TEM irradiation experiments.

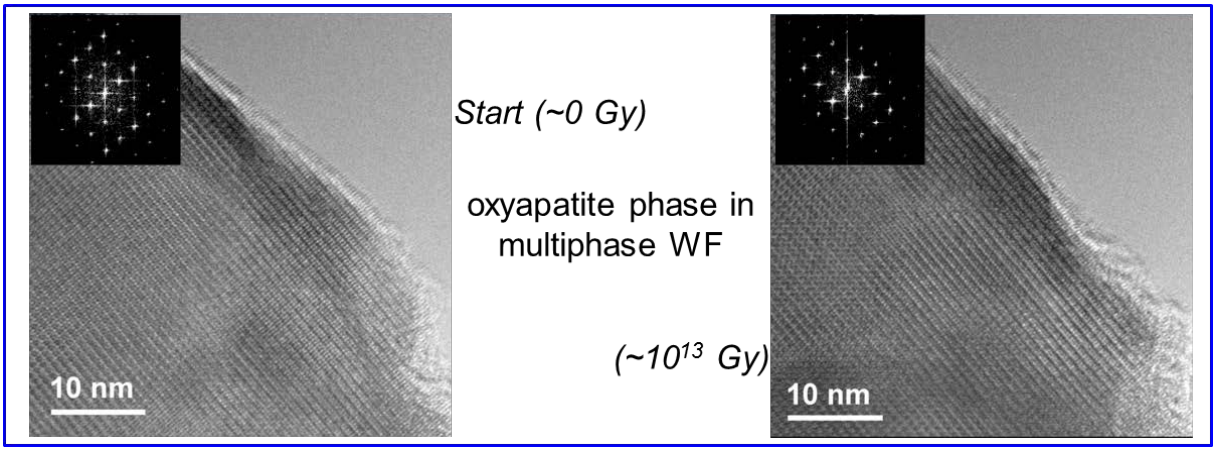

(a)

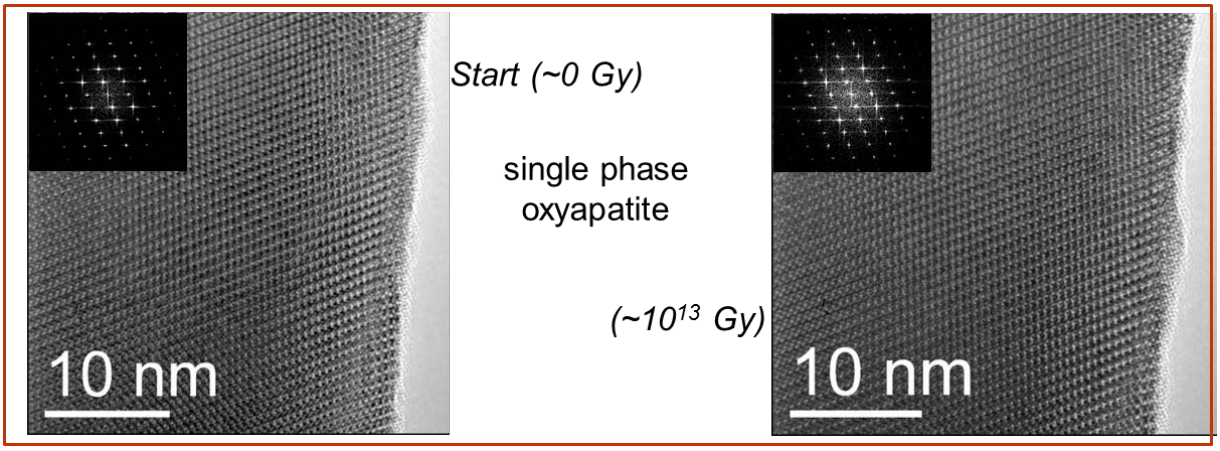

(b)

Figure 10. (a) High resolution transmission electron microscopy image of oxyapatite phase in multiphase glass ceramic Mo-6.25 before (left) & after (right) electron irradtion including FFT diffraction; (b) High resolution transmission electron microscopy image of single phase oxyapatite before (left) & after (right) electron irradtion including FFT diffraction.

4.3 Radiation stability test on single phase oxyapatite under Kr irradiations at different temperatures

To simulate decay heats representative of different radionuclide loadings of a waste form and evaluate the temperature effect on radiation stability of oxyapatite phase. 600 keV Kr ion irradiations were performed at 250 °C and radiation damage results were compared with room

temperature irradiations. In Figure 11, XRD results show that irradiation-induced amorphization is observed in Kr irradiated single phase oxyapatites (left) at room temperature oxyapatite (see arrows); however, no amorphization observed at elevated temperature (250 °C) Kr irradiation (right) suggests the thermal recovery of radiation damage.

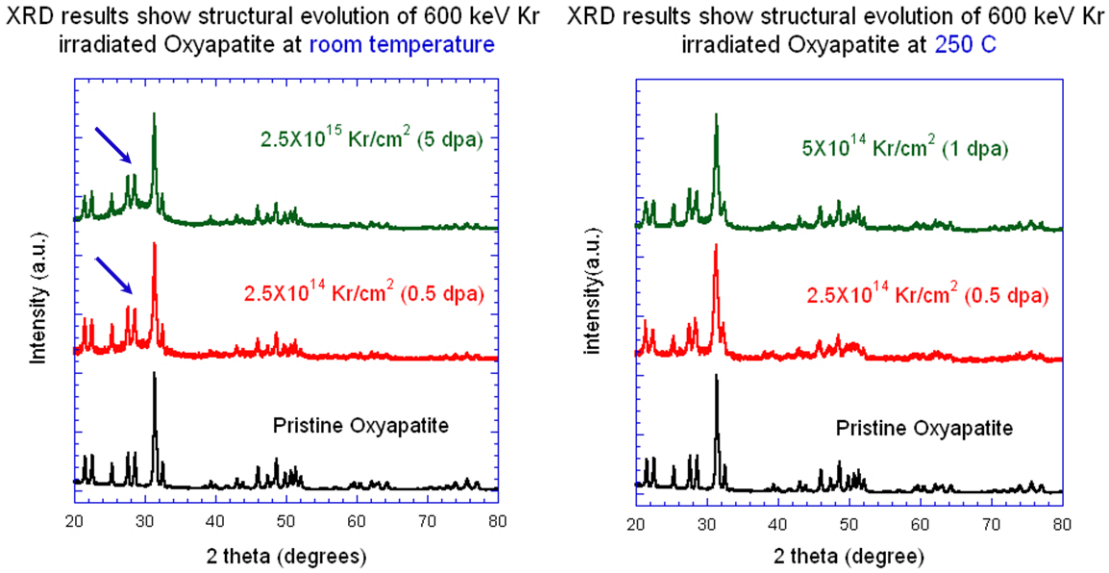

(a) (b)

Figure 11. XRD results of single phase oxyapatite before and after 600 keV Kr irradiations at different temperatures (a) room temperature, (b) 250 °C.

4.4 Radiation stability test on single phase oxyapatite under He irradiations at different temperatures

Heavy ions (e.g. Kr) are used to simulate energetic recoil nuclei interaction which involves ballistic processes, especially for alpha decay; while light ions (e.g. He) are used to study the role of ionization on the structural evolution in crystalline structures. In this task, single phase oxyapatites were irradiated with 5 MeV He (alpha) and 200 keV He ions at room temperature and elevated temperature (250 °C). XRD results in Figure 12 shows that no irradiation-induced amorphization is observed in single phase oxyapatites under 5 MeV He (left) and 200 keV He irradiations (right) at room temperature and elevated temperature. It suggests that oxyapatite exhibits strong radiation tolerance under ionization damage.

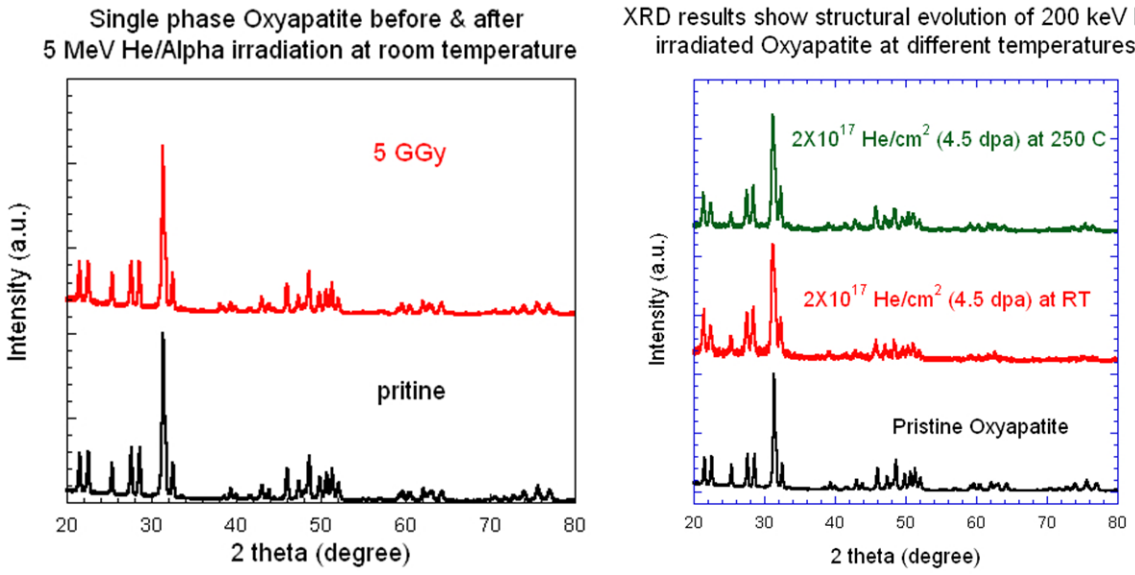

(a) (b)

Figure 12. (a) XRD results of single phase oxyapatite before and after 5 MeV He irradiations at room temperature; (b) XRD results of single phase oxyapatite after 200 keV He irradiations at room temperature and 250 °C.

Radiation stability on oxypatatite phase in multiphase glass ceramic and corresponding single phase oxyapatite has been investigated upon 5 MeV He, 200 keV He, 600 keV Kr ion irradiations, and *in-situ* electron irradiation in TEM at various temperatures. The oxyapatite phase in multiphase waste form shows the similar radiation response to the corresponding single phase under the similar radiation conditions. These ion beam irradiation results also indicate that oxyapatite phase is radiation tolerant to ionization damage due to the β–particles and γ-rays, but susceptible to amorphization under ballistic displacement damage from recoil nuclei effects. Ion irradiations at 250 °C reveal that Oxyapatite exhibits a very good ability to anneal defects so that durability is not compromised even under high radiation fluxes experienced during storage or disposal for waste form application. *In-situ* electron irradiation results indicate that the oxyapatite phase retains its crystalline structure after a radiation dose of 10^{13} Gy, which is much higher than 1000 y of self-irradiation dose for a highly loaded Cs/Sr waste form.

5. Future work

LANL will focus on characterization and testing procedures on glass ceramics from the test matrix and melter testing to further develop and mature the glass ceramic waste form. FY15 activities include: (1) characterize glass ceramic waste forms from PNNL and INL using micro-

X ray diffraction, TEM/STEM, and nano-indentation techniques, (2) test their corrosion behavior after irradiation by the product consistency test and ion beam irradiation techniques.

References

[1] A. T. Nelson, J. V. Crum, and M. Tang, *J. Amer. Ceram. Soc.*, 97 [4] (2014) 1177.

[2] M. Tang, A. Kossoy, G. Jarvinen, J. Crum, L. Turo, B. Riley, K. Brinkman, K. Fox, J. Amoroso, J. Marra, *Nucl. Instr. and Meth. B*, 326 (2014) 293.

[3] R. Bros, J. Carpena, V. Sere and A. Beltritti, *Radiochimica Acta*, 74 (1996) 277.

[4] H. Hidaka, K. Takahashi and P. Holliger, *Radiochim. Acta*, 66(67) (1994) 463.

[5] D. J. Wronkiewicz, S. F. Wolf and T. S. Di Santo, in Scientific Basis for Nuclear Waste Management XIX, ed. W. M. Murphy and D. A. Knecht, *Mater. Res. Soc. Sym. Proc.* Vol. 412, Pittsburgh, 1996, p. 345

[6] J. Crum, L. Turo, B. Riley, M. Tang, A. Kossoy-Simakov, *J. Am. Ceram. Soc.*, 95 (2012) 1297.

[7] W. J. Weber, Y. Zhang, H. Xiao, and L. M. Wang, *RSC Advances*, 2 (2012) 595.

[8] W. J. Weber, *J. Am. Ceram. Soc.*, 65 (1982) 544.

[9] L. M. Wang and W. J. Weber, *Philos. Mag.* A, 79 (1999) 237.

[10] J.F. Ziegler, J.P. Biersack, U. Littmark, The Stopping and Range of Ions in Solids, Pergamon Press, New York, 1985.

[11] W.J. Weber, A. Navrotsky, S. Stefanovsky, E.R. Vance and E. Vernaz, *MRS Bull*. 34 (2009) 46.